electronics

Article

Interrupted-Sampling and Non-Uniform Periodic Repeater Jamming against *m*DT-STAP System

Jiyang Li *, Xiaohu Duan, Jia Li and Peng Bai

Fundamentals Department, Air Force Engineering University, Xi'an 710051, China
* Correspondence: lijiyang1991@163.com

Abstract: The difference between sampling data and detection data can degrade the performance of space-time adaptive processing (STAP). A jamming algorithm with a non-uniform periodic repeater based on interrupted-sampling is proposed against the reduced dimensional space-time adaptive processing (STAP) system for the first time. Firstly, the model of m-bins doppler transform (mDT) STAP training and processing signal samples is described. Then, the method of false targets generated by the non-uniform periodic repeater is analyzed theoretically based on the principle of interrupted-sampling. The simulation shows that numerous false targets with different amplitude and intervals can be generated by changing the retransmitted parameters. The independent identical distribution (IID) of system sample data can be destroyed after these false targets are received by the radar system, and the main lobe will be distorted when the system's adaptive weight vector is formed. The processing performance of the mDT-STAP system is seriously degraded. The jamming method proposed based on interrupted-sampling and the non-uniform periodic repeater offers great potential for the interference research on STAP in real conditions.

Keywords: reduced dimension; space-time adaptive processing; interrupted-sampling; non-uniform repeater; jamming

check for updates

Citation: Li, J.; Duan, X.; Li, J.; Bai, P. Interrupted-Sampling and Non-Uniform Periodic Repeater Jamming against *m*DT-STAP System. *Electronics* **2023**, *12*, 152. https://doi.org/10.3390/electronics12010152

Academic Editors: Yangyang Dong, Hua Chen and Fangqing Wen

Received: 14 November 2022
Revised: 24 December 2022
Accepted: 26 December 2022
Published: 29 December 2022

1. Introduction

STAP is one of the key technologies of the new generation of high-performance radar. To improve the accurate detection of targets and suppress clutter, noise and jamming, the independent identical distribution sample data is processed jointly by the STAP system in the time domain and space domain [1–4]. Compared with the full-dimensional STAP system, the mDT-STAP system has the characteristics of a small amount of calculation and small demand for training samples because m time-domain channels are selected for filtering. In addition, clutter and jamming can be suppressed effectively in both positive side-looking and non-positive side-looking mDT-STAP airborne systems. Moreover, the mDT method is not sensitive to array error [5,6].

Consuming system degrees of freedom is a strategy against the STAP system. The performance of the STAP system will decline significantly when the degree of freedom of the system is not large enough to eliminate jamming [3]. In 2013, a way to occupy the feature space of the system by generating dense interference signals is proposed by Y. Zhang et al. [7]. However, a large number of jammers are required, which reduces the possibility of implementation. Clutter scattering jamming is investigated by Q. Zhou's team from 2016 to 2021, which means that the radar is scattered by the wideband jamming signal after throwing to the ground [8–10]. In this way, numerous space-time degrees of freedom will be occupied by the generated scattering jamming. However, clutter scattering jamming is greatly affected by terrain factors and the communication environment between multiple signal sources. Additionally, the scattered wave can be received weakly by radar because of the small energy.

To construct a heterogeneous environment is another mainstream strategy. Training samples and detection samples are two kinds of data in the STAP system. The jamming information in detection samples data is estimated by training the sampling data. A heterogeneous environment can be generated by constructing differences between sampling data and detection data [11]. In this way, the jamming information of the detection data cannot be eliminated by training the sampling data. In 2012, a rapidly changing signal environment is proposed by X.Tang et al. [12]. However, the implementation method is undefined. In 2016, modulating and transmitting the pulse compression signal to generate false target information in the training samples is proposed by C. Liu et al. However, the number and position of false pulses cannot be set independently [13]. In 2020, a jamming algorithm based on time-delay aliasing transmission against the reduced dimension STAP is investigated by Y. Zhao et al. [14]. In 2021, a slow-time-frequency-modulation jamming method is proposed by X. Chen. Numerous false targets with controllable distribution can be generated by the above two methods [15]. The above retransmitting jamming methods are based on the full pulse modulation. However, when the radar pulse width is large, the limited shape and volume of the jammer sometimes cannot meet the required transceiver isolation. When the anti-jamming measures of frequency agility and frequency diversity are used by the radar, the false target generated by retransmitting will jump at multiple range points, thus being recognized by the radar [16].

In addition, the false targets generated by the above retransmitting methods have a certain regularity in amplitude and interval and are easily recognized and eliminated by radar system.

In this paper, we proposed a jamming algorithm of a non-uniform periodic repeater based on interrupted-sampling [17–20] against the *m*DT-STAP system by constructing an heterogeneous environment for the first time. The method can generate numerous false targets with different amplitudes and intervals, which, in creating heterogeneous conditions for a radar system, is easier than direct retransmitted jamming and uniform periodic repeater jamming. Moreover, the jamming method, based on DRFM system, can be applied to the jamming equipment isolated by the transceiver system and working at the same time. Compared with the full-sampling, the proposed method does not need to change the instantaneous transmission power to generate false targets with different amplitude in the process of non-uniform retransmitting, which reduces the hardware system complexity and the energy loss caused by frequent power switching. The jamming parameter modulation can be completed in the digital domain; it requires little difference in hardware when compared with the widely used jamming equipment based on DRFM. The engineering implementation of this method is not difficult, and only part of the software codes needs to be changed. Therefore, the proposed jamming method on interrupted-sampling and the non-uniform periodic repeater offers great potential for the jamming research on STAP in real conditions.

The remainder of this paper is organized as follows. The signal model of *m*DT-STAP is introduced in Section 2. In Section 3, the interrupted-sampling principle and counter measure scenario are firstly. Then, the jamming method of the non-uniform periodic repeater based on interrupted-sampling is illustrated in detail. After that, Section 4 provides simulation results to verify the performance of the proposed method. Finally, Section 5 summarizes this paper.

2. Signal Model of *m*DT-STAP

The target information is contained in the detection sample. The covariance matrix of the detection sample $\boldsymbol{R}_{\mathbf{u}}$ is composed of clutter covariance matrix $\boldsymbol{R}_c$, jamming covariance matrix $\boldsymbol{R}_j$ and noise covariance matrix $\boldsymbol{R}_n$, which can be expressed Equation:

$$\boldsymbol{R}_u = E\left\{\boldsymbol{x}\boldsymbol{x}^H\right\} = \boldsymbol{R}_c + \boldsymbol{R}_j + \boldsymbol{R}_n \tag{1}$$

where $\boldsymbol{x}$ represents the received data. When clutter is suppressed by system suppresses, the auxiliary range unit echo data is used to estimate $\boldsymbol{R}_u$ to protect the target information from cancellation. This can be expressed Equation (2):

$$\hat{\boldsymbol{R}}_{SCM} = \frac{1}{L}\sum_{l=1}^{L} \boldsymbol{x}_l \boldsymbol{x}_l^H \tag{2}$$

$\{\boldsymbol{x}_l\}(l = 1, 2, \cdots L)$ represents data samples from different distance units. Under the IID condition, when $\{\boldsymbol{x}_l\}$ has the same covariance matrix as the detection sample, the estimation of $\boldsymbol{R}_u$ is unbiased. According to the Reed, Mallett, Brennan (RMB) criterion [1], the number of IID samples is required to be at least twice the dimension of the $\hat{\boldsymbol{R}}_{SCM}$ to make the SCNR of the system after filtering clutter less than 3 dB. However, the dimension of full-dimensional STAP is so large that many samples are required. The dimension reduction space-time adaptive technology is selected for processing.

*m*DT-STAP [21] is a widely used dimensionality reduction algorithm, and the model is shown in Figure 1. The data received by the system is sent to the forward filter. The received signal is preprocessed by doppler filtering with time window to remove the influence of clutter signal outside the doppler passband, and a large number of input data samples can be converted into relatively few samples [22]. To balance the performance, computation and the number of samples, we select three doppler channels for forward filtering [23]. The preprocessing matrix $\boldsymbol{T}$ can be obtained by a priori knowledge estimation of clutter distribution. It is the balance between the number of samples and the amount calculated by the system.

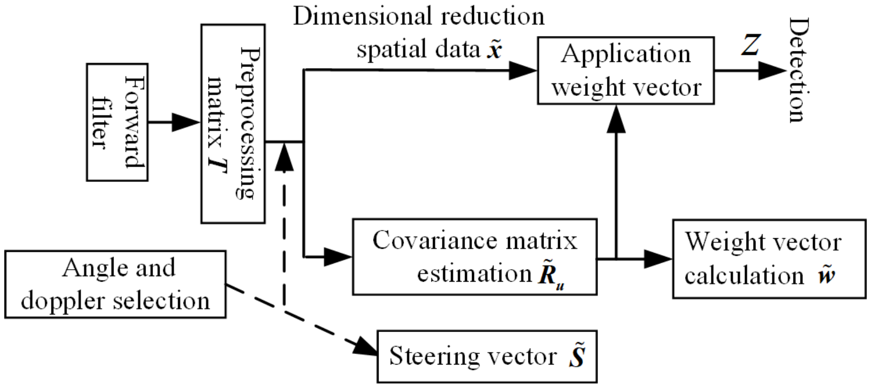

Figure 1. Process model of *m*DT-STAP.

The data received by the system can be divided into two types of samples: training samples and detection samples, as shown in Figure 2.

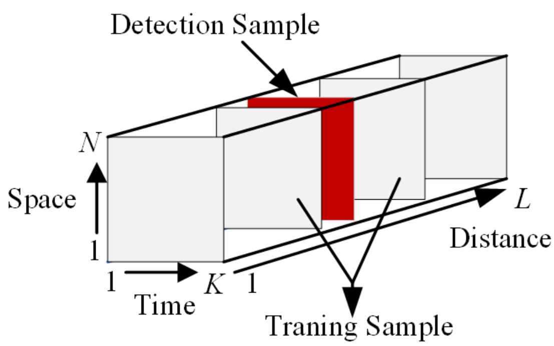

Figure 2. Input data of *m*DT-STAP.

The input data of the distance unit to be detected is $NK \times 1$ dimensional space-time sample $x(l)$, where N represents the number of array elements and K represents the number of pulses. In Equation (3), the data is converted into $D \times 1$ dimensional vector. The number of training samples is reduced to $D(D << NK)$.

$$\widetilde{\boldsymbol{x}}(l) = \boldsymbol{T}^H \boldsymbol{x}(l) = \alpha \widetilde{\boldsymbol{s}} + \widetilde{\boldsymbol{x}}_u \tag{3}$$

where α is the amplitude of the target signal and $\widetilde{\boldsymbol{s}}$ and $\widetilde{\boldsymbol{x}}_u$ represent the target steering vector and clutter data after dimensionality reduction, respectively. Thus, the clutter covariance matrix $\widetilde{\boldsymbol{R}}_{\boldsymbol{u}}$ of the distance unit to be detected can be expressed in Equation (4):

$$\widetilde{\boldsymbol{R}}_u = \frac{1}{L} \sum_{l=1}^{L} \boldsymbol{x}_u(l) \boldsymbol{x}_u{}^H(l) = \boldsymbol{T}_{mDT}{}^H \hat{\boldsymbol{R}}_u \boldsymbol{T}_{mDT} \tag{4}$$

where

$$\boldsymbol{T}_{\mathrm{mDT}} = [\boldsymbol{T}_t(f_{d,k-[m/2]}) \cdots \boldsymbol{T}_t(f_{d,k}) \cdots \boldsymbol{T}_t(f_{d,k+[m/2]})] \otimes \boldsymbol{I}_N. \tag{5}$$

$f_{d,k}$ represents the center frequency of the k-th doppler channel, K represents the k-point FFT, and m means the number of doppler channels selected. $k - [m/2], \ldots, k, \ldots, k + [m/2]$ express a doppler filter bank composed of m doppler filters. m is usually an odd number. $\boldsymbol{I}_{\mathrm{N}}$ means N identity matrix. $\otimes$ expresses the Kronecker product.

The optimal solution of the adaptive weight vector $\widetilde{\boldsymbol{w}}$ of the system [22] can be obtained by the Lagrange multiplier method in Equation (6):

$$\widetilde{\boldsymbol{w}}_{m\mathrm{DT}}(f_{d,k}, f_{sp}) = \frac{\widetilde{\boldsymbol{R}}_{m\mathrm{DT}}^{-1} \widetilde{\boldsymbol{s}}_{m\mathrm{DT}}}{\widetilde{\boldsymbol{s}}_{m\mathrm{DT}}^{\mathrm{H}} \widetilde{\boldsymbol{R}}_{m\mathrm{DT}}^{-1} \widetilde{\boldsymbol{s}}_{m\mathrm{DT}}} \tag{6}$$

where $\widetilde{\boldsymbol{R}}_{m\mathrm{DT}} = \boldsymbol{T}_{m\mathrm{DT}}^{\mathrm{H}} \hat{\boldsymbol{R}}_u \boldsymbol{T}_{m\mathrm{DT}}, \widetilde{\boldsymbol{s}}_{m\mathrm{DT}} = \boldsymbol{T}_{m\mathrm{DT}}^{\mathrm{H}} \boldsymbol{s}$ and the final output of the system can be obtained as follows:

$$z = \widetilde{\boldsymbol{w}}_{m\mathrm{DT}}^{\mathrm{H}} \widetilde{\boldsymbol{x}}(l) = (\boldsymbol{T}_{m\mathrm{DT}} \widetilde{\boldsymbol{w}}_{m\mathrm{DT}})^{\mathrm{H}} \boldsymbol{x}(l). \tag{7}$$

The training samples required by the mDT-STAP system must meet the IID condition. Clutter and noise information are included in the training samples. In addition to clutter and noise, target information is also included in the samples to be detected. When the jamming similar to the target information is applied to the training sample, the IID condition of training samples is destroyed; that is to say, jamming information will be included in the $\widetilde{\boldsymbol{R}}_u$ estimated by the training samples. According to Equation (6), the weight vector $\hat{w}$ obtained from $\widetilde{\boldsymbol{R}}_u$ will be distorted.

3. Principle of Jamming Method

3.1. Interrupted-Sampling Principle

The interrupted-sampling can be used to realize the time-sharing mechanism of the jammer. When a large time width radar signal is intercepted, a small segment is sampled with high fidelity and processed and retransmitted immediately. Then, the next segment is sampled, processed and retransmitted. The sampling and retransmission work alternately in time-sharing until the end of the large time width signal.

The principle of interrupted-sampling can be shown in Figure 3. Firstly, when the jammer is in the interception window (WR is at high level), the jammer can detect the intercepted radar signal. Then, when the sampling detection pulse DET is at high level, DRFM is used to store the sampled signal until the sampling signal pulse width is greater than the intermittent time τ. Ultimately, the jamming transmission strobe pulse JT is turned to high level, WR is turned to low level and the stored data will be transmitted. T_j is the length of jamming window.

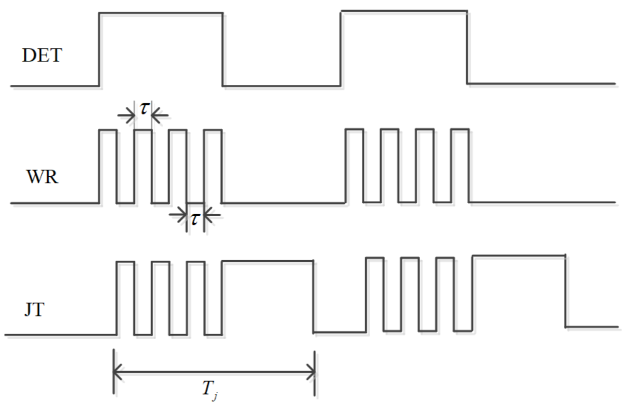

Figure 3. Schematic diagram of interrupted-sampling.

Interrupted-sampling pulse signal $c(t)$ can be expressed by Equation (8):

$$c(t) = rect(\frac{\tau}{T}) \sum_{n=-\infty}^{\infty} \delta(t - nT_s). \tag{8}$$

Through the ambiguity function [17], the output expression of interrupted-sampling and the transmitting signal after pulse compression can be expressed in Equation (9):

$$y_s(t) = \sum_{n=-\infty}^{\infty} y_{sn}(t) = \sum_{n=-\infty}^{\infty} A_n \sin\mathrm{c}\{T[k_f(t - T_r) + nf_s](1 - \frac{|t - T_r|}{T})\} \bullet \exp(\mathrm{j}2\pi n f_s t) \tag{9}$$

where $\sin\mathrm{c}(x) = \sin(\pi x)/\pi x$, $y_s(t)$ can be seen as the result of the synthesis of a series of target echoes with different frequency shift nfs and time delay $T_r = T_d + T$ after matched filtering, and T_d is the time delay of jammer.

According to the characteristics of the sinc function [18], the maximum amplitude of the n-th order signal component can be expressed by Equation (10):

$$|y_{sn}(t_{\max})| = \tau f_s \sin\mathrm{c}(n\tau f_s)(1 - \frac{nf_s}{B}). \tag{10}$$

The position where the maximum amplitude occurs can be expressed by Equation (11):

$$T_{sn\_\max} = \frac{-nf_s}{k_f} + T_r = \frac{-nf_s T}{B} + T_r. \tag{11}$$

When $n = 0$ and $t = T_r$, the maximum amplitude can be expressed by Equation (12):

$$|y_s(t)| = \tau f_s. \tag{12}$$

It can be seen that the interrupted-sampled and transmitted signal will generate the same main false target as the echo signal of the real target after matched filtering. Its amplitude is proportional to the duty cycle of the sampling pulse $c(t)$.

3.2. Countermeasure Scenario

To protect the target, a penetration formation is formed by a small RCS jammer accompanying the target movement during the target movement. The jammer moves in the direction close to the radar in front of the target. The reconnaissance system is used to obtain the radar signal and carry out appropriate modulation to achieve the purpose of suppressing multiple false targets against the radar.

Target detection by mDT-STAP requires training samples to meet IID conditions, training samples to contain clutter and noise information and the number of distance units to be detected. However, when the false targets are added to the training unit, the signal no longer meets the IID condition.

The geometric configuration of radar and jammer is shown in Figure 4. The uniform linear array is used by radar antenna. The carrier moves at a velocity v_a in the altitude of H. Azimuth and pitch angles of the antenna beam are denoted by φ and θ, respectively. The incident cone angle of the clutter scatterer relative to the array antenna is expressed by ψ, and the included angle between the array antenna and the navigation direction of the carrier is represented by α.

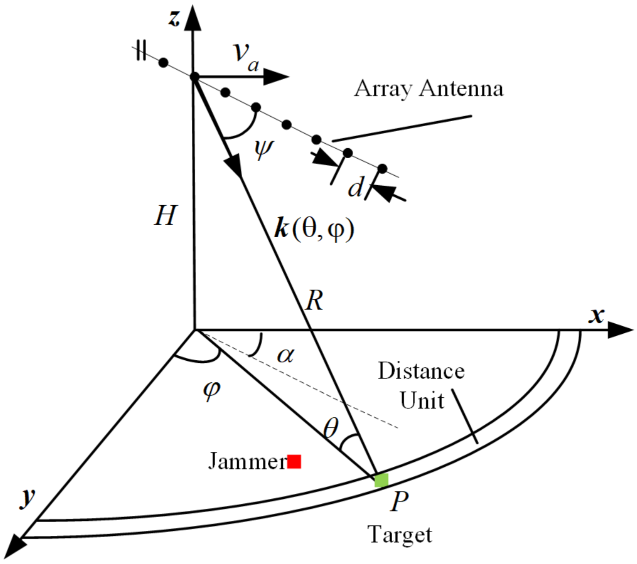

Figure 4. Geometric configuration of radar and jammer.

3.3. The Proposed Jamming Method

The main idea to achieve multiple false targets jamming is to form a column of false targets with amplitude decreasing to both sides successively before and after the true target by the escort support jammer, as shown in Figure 5.

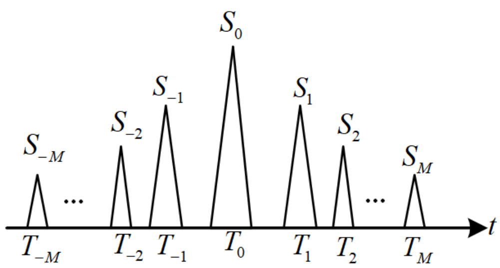

Figure 5. Geometric configuration of radar and jammer. (The distribution of false targets).

As can be seen form Figure 5, as the center of S_0, the amplitude of false targets S_i on both sides decreases gradually. To ensure that there is at least one jamming target in the left and right reference range units of the target, the following conditions in Equation (13) must be met:

$$\Delta R \leq L/2 \tag{13}$$

where ΔR is the distance between two targets, and L is the length of reference unit.

The interrupted-sampling and non-uniform periodic repeater jamming is shown in Figure 6. It is employed to ensure that the number of false targets is sufficient and has non-uniformity.

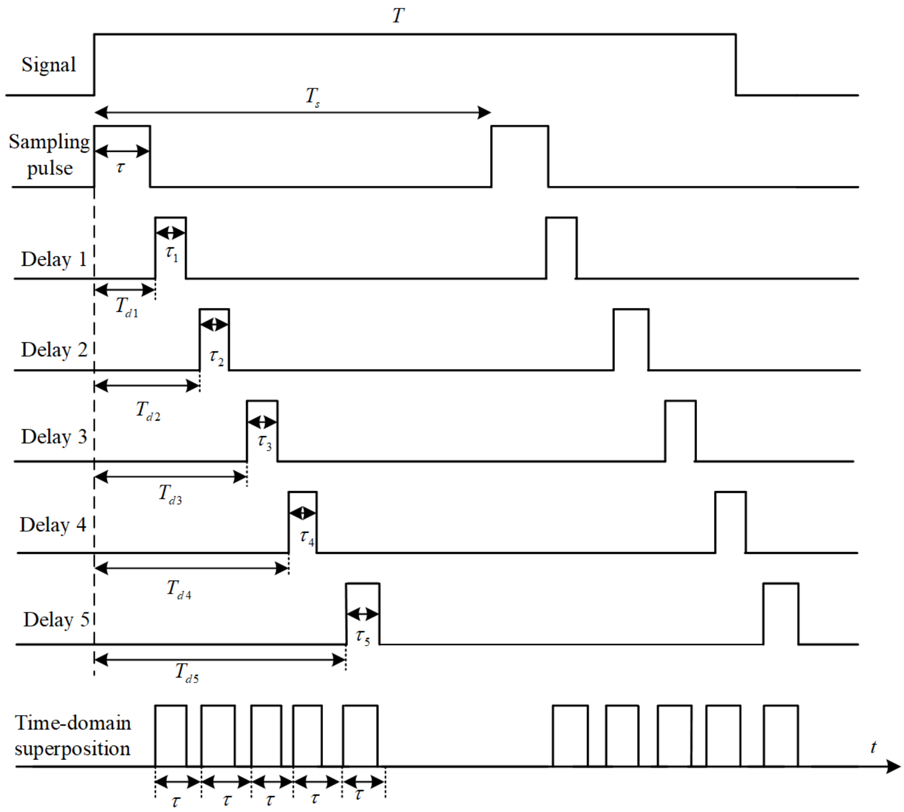

Figure 6. Interrupted-sampling and non-uniform periodic repeater jamming.

As it can be seen from Figure 6, the radar pulse width T is an integral multiple of the interrupted-sampling period T_s. The number of transmitted pulses in a sampling period is equal to the number of false targets. The delay time of the false target is expressed in T_{dm}. The next transmitted pulse will be delayed one sampling pulse τ width based on the previous transmitted time; that is to say, $T_{dm+1} - T_{dm} = \tau$. When the duration of transmitted pulse is τ, that is

$$\tau_1 = \tau_2 = \cdots = \tau_m = \tau, \tag{14}$$

the interrupted-sampling and uniform periodic repeater jamming is available.

The output expression of the first transmitted interference pulse after sampling can be expressed by Equation (15):

$$y_1(t-\tau_1) = s(t)rect(\frac{t}{\tau_1})\sum_{n=-\infty}^{\infty}\delta(t-nT_s-T_{d1}) \tag{15}$$

where $s(t)$ is used to dispel the radar signal. The result of time domain addition can be expressed by Equation (16):

$$y(t) = \sum_{n=1}^{m} y_n(t-\tau_n). \tag{16}$$

As can be seen from Equation (16), the non-uniform repeater jamming can generate multiple main false targets with different amplitudes in the radar receiver. The amplitude of each false target is proportional to the width of the transmitted pulse, and the interval between false targets is τ_m.

To achieve jamming effect, the following parameters of the false target need to be determined:

- Sampling pulse width τ:

The sampling pulse width τ and the length of radar CFAR detection reference unit shall meet the relationship in Equation (17):

$$\tau \geq L/2c \tag{17}$$

where L is the length of radar detection reference unit;

- Retransmitting delay time T_{d}:

As can be seen from Figure 6, the delay time of the retransmitted pulse is related to the distance between the jammer and the target. The distance rm between the m-th false target and true target can be expressed as Equation (18):

$$r_m = (M-m)L/2 + L/4 \tag{18}$$

where M is the number of false targets. The delay time of the false target generated by each retransmission can be expressed by Equation (19):

$$T_{dm} = \frac{2R_{jt}}{c} + 2(M-m-\frac{1}{2})\tau \tag{19}$$

where R_{jt} is used to indicate the distance between the jammer and the true target. To obtain sufficient transmitting time, the distance between the jammer and the true target can be expressed by Equation (20):

$$R_{jt} \geq r_m. \tag{20}$$

Therefore, T_{dm} shall meet the conditions shown in the Equation (21):

$$T_{dm} \geq (M-m)(2+\frac{L}{c}) + \frac{L}{2c} - \tau; \tag{21}$$

- Retransmitting pulse width τ_m:

As can be seen from Figure 5, the amplitude Am of the false target is proportional to the width τ_m of the retransmission pulse. Its amplitude decreases gradually from the inside to the outside, which means that the width of the retransmission pulse gradually narrows from the inside to the outside:

$$\tau_M < \cdots < \tau_1 \leq L/2c \tag{22}$$

$$\frac{\tau_{m-1}}{\tau_m} = \frac{A_{m-1}}{A_m} = \sqrt{\frac{\chi_{m-1}}{\chi_m}} \tag{23}$$

where χ_m indicates the signal to noise ratio of the false target. As the maximum distance between the main and false targets is L, the maximum retransmitting pulse width is $L/2c$;

- Sampling period T_{s}:

One sampling and M times retransmitting are performed in a sampling period. Therefore, after the sampling pulse width τ_m is determined, the sampling period length can be expressed by Equation (24):

$$T_s = T_{d1} + M\tau \tag{24}$$

where the sampling pulse width τ is merged into the leftmost false target delay time T_{d1}.

4. Simulations and Analysis of Jamming Effect on *m*DT-STAP

In this section, simulation results are used to verify the performance of the proposed method. The general case airborne radar parameters shown in Table 1 are carried out.

Table 1. Radar system parameters.

Parameter	Value
Carrier height	3 km
Carrier velocity	125 m/s
Carrier frequency	6 GHz
Pulse width	20 μs
Pulse repetition frequency	10 KHz
Sampling frequency	100 MHz
Pulse accumulation number	20
Number of array element	16

- The distance ΔR between two false targets is equal to half of the length L of the radar CFAR detection reference range unit. The sampling pulse width τ is equal to $L/2c$.

In the first simulation, to evaluate the accuracy of the jamming estimates, the results are illustrated in this subsection. Figure 7a shows the result after matched filtering by the jamming with direct retransmission, and Figure 7b,c provides the jamming estimated after matched filtering by the interrupted-sampling with the uniform and non-uniform periodic repeater, respectively.

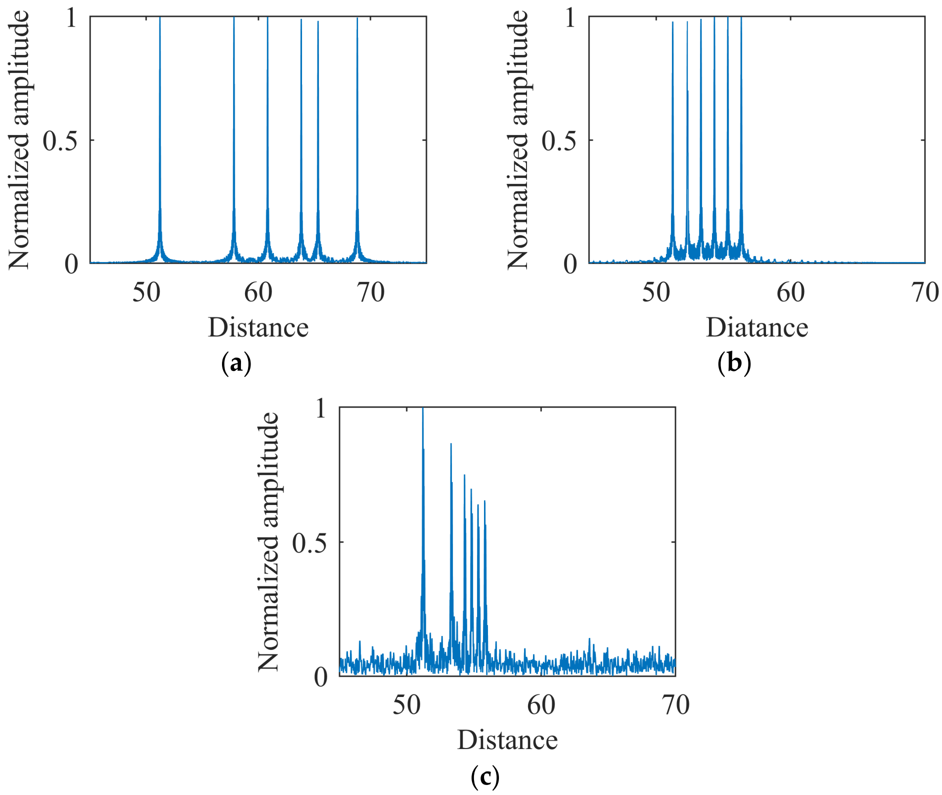

Figure 7. Jamming estimated based on different methods: (**a**) direct retransmitted jamming; (**b**) interrupted-sampling and uniform periodic repeater jamming; (**c**) interrupted-sampling and non-uniform periodic repeater jamming; (**a**) T_d = 13, 19, 25, 28, 35 μs and $\tau = \tau_m$ = 20 μs; (**b**) T_d = 2, 4, 6, 8, 10 μs, and $\tau = \tau_m$ = 5 μs; (**c**) T_d = 3, 6, 7, 8, 10 μs, τ = 5 μs and τ_m = 5, 3, 2, 1, 1 μs.

- As shown in Figure 7a, after the intercepted signal is stored in full pulse, it is delayed for five times and five realistic false targets are generated. Considering the retransmitted delay time T_d of jammer with signal pulse width, the generated false targets are at least 33 μs, 39 μs, 45 μs, 48 μs and 55 μs behind the true target echo, respectively. The false targets are 5 km (No. 59 in distance), 5.9 km (No. 62), 6.8 km (No. 65), 7.2 km (No. 66) and 8.3 km (No. 69) behind the true target (No. 51) in distance, respectively.

Because the distance between the true and false targets are too large, the false targets may not be in the radar range gate.

- It can be seen from Figure 7b that, after interrupted-sampling, five false targets are generated by the retransmitting signal five times with the same pulse width. The interrupted-sampling and uniform periodic repeater can solve the problem that the distance between the false target and the true target is too large. However, the distribution of the generated false target group shows a certain regularity with the fixed interval and amplitude. The false target group can be easily identified by radar system.
- Figure 7c shows that five false targets are generated by the retransmitting signal five times with the different pulse width after interrupted-sampling. The non-uniform periodic repeater can generate false target groups with different amplitude and intervals by changing the retransmitted pulse width.
- The second simulation focuses on the escort support jamming result of the interrupted-sampling and non-uniform periodic repeater jamming against the *m*DT-STAP system. The azimuth angle of the moving target on the ground relative to the radar is 45° and the elevation angle is −23°. The velocity of target v_t = 60 m/s. The azimuth distribution of clutter ranges from −90° to 90° and CNR = 60 dB. The *m*DT-STAP system selects data from three adjacent doppler channels for processing, i.e., m = 3. The azimuth angle of the escort support jammer with the relative to the radar is 57° and the elevation angle is −15°. The velocity of jammer v_j = 42.3 m/s. The interrupted-sampling pulse width τ is 4 µs, the delays T_d are 3 µs, 6 µs and 9 µs, respectively, and the widths of the retransmission pulse τ_m are 3 µs, 2 µs, 2 µs, respectively.
- The false targets can fall into detection samples or training samples by controlling the jammer position, the amount of delay T_d and the transmitted pulse width τ_m. The different processing results of the 3DT-STAP with the proposed jamming method are shown in Figures 8 and 9.
- Figure 8 shows the processing result when the false targets are contained in the detection samples of the 3DT-STAP. As can be seen from Figure 8a, the real target in the distance dimension is surrounded after 3DT-STAP processing. Because there is coherence between radar signal and jamming signal which exists in the detection samples. When the true target is detected, the false target is also detected. As shown in Figure 8b, the azimuth and doppler information of the target cannot be accurately identified due to the existence of false targets in the space-time two-dimensional response. This indicates that the false alarm probability of the radar system will be increased when the non-uniform jamming exists in the detection samples.

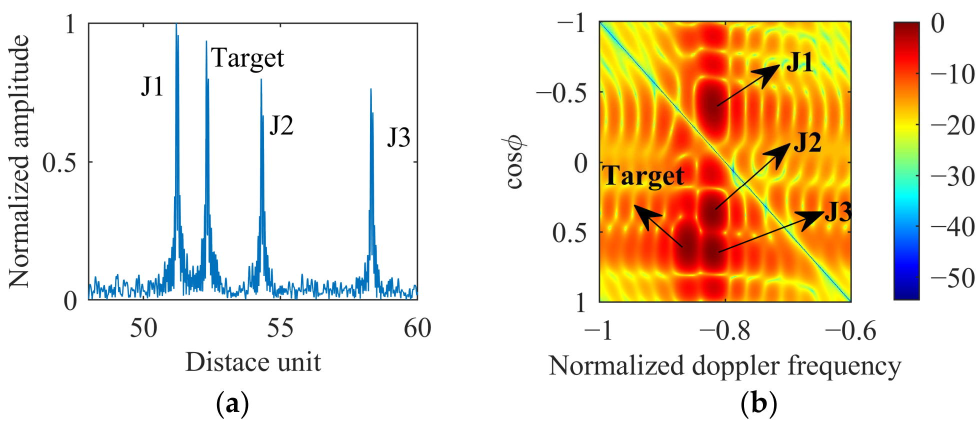

Figure 8. Processing result of detection samples containing false targets: (**a**) radar echo data after 3DT-STAP processing; (**b**) two-dimensional response after 3DT-STAP processing.

- Figure 9 shows the processing result when the false targets are contained in the training samples of the 3DT-STAP. As can be seen from Figure 9a, the real target in the distance dimension is eliminated after 3DT-STAP processing. Because the false targets contained in training samples are coherent with the target in detection samples, the real target, recognized by radar as jamming, is eliminated. As shown in Figure 9b, the false targets included in the training sample cause the 3DT-STAP processor to form a null at the two-dimensional power spectrum of the direction doppler image. The azimuth and doppler information of the target cannot be obtained after 3DT-STAP processing.

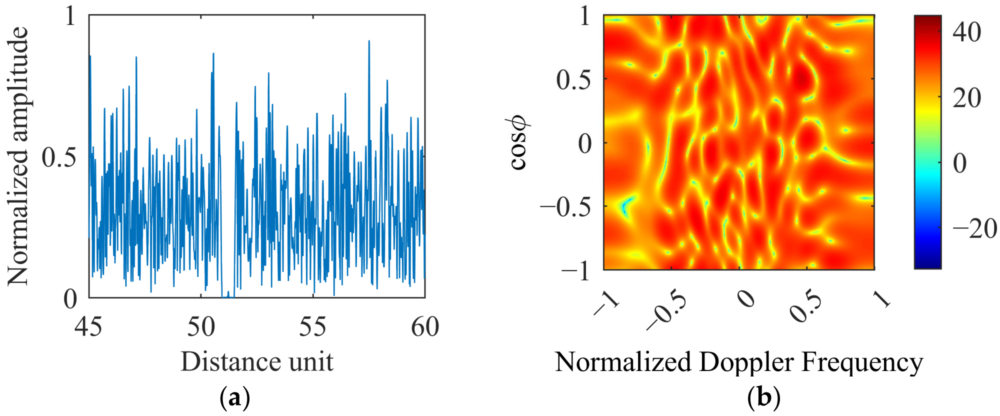

Figure 9. Processing result of training samples containing false targets: (**a**) radar echo data after 3DT-STAP processing; (**b**) two-dimensional response after 3DT-STAP processing.

Figure 10 shows the normalized improvement factors of the system under different jamming conditions. Condition 1 shows the system performance when false targets are contained in training samples. The system can get samples with clutter, noise and false targets to train. The targets in the detection samples can be regard as false targets, which can cause targets to be eliminated. Moreover, the non-uniform distribution of training samples will lead to the broadening of clutter suppression nulling, resulting in the reduction of output SNR and the degradation of system performance. As can be seen form condition 2, the improvement factors of the system have hardly changed; when no jamming exists or false targets are contained in detection samples, the system can only get samples with clutter and noise to train. Only clutter and noise are eliminated and the system cannot identify and eliminate false targets, which increases the false alarm rate of the system.

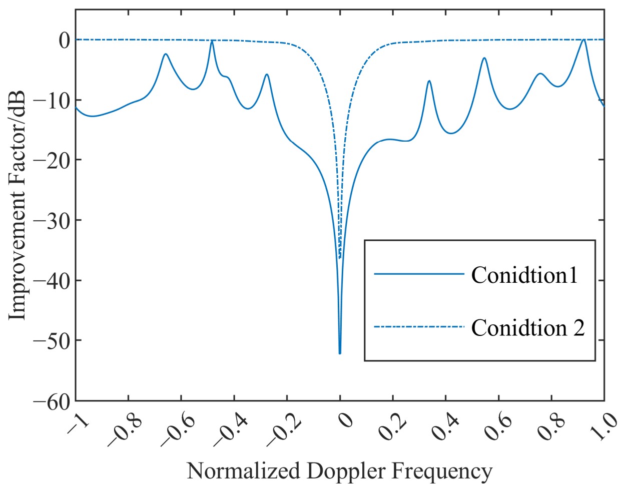

Figure 10. Normalized improvement factors of the system. Condition 1 means false targets are contained in training samples; Condition 2 means false targets are contained in detection samples.

5. Conclusions

A jamming method employing a non-uniform periodic repeater based on interrupted-sampling is presented to against mDT-STAP. The proposed method constructs a non-uniform signal environment by non-uniform periodic repeater retransmitting and retains the number of false targets to the maximum extent. This method can generate false targets with different amplitudes and intervals at the algorithm level, without changing the instantaneous transmit power of the jammer, thus reducing the hardware system complexity and the energy loss caused by frequent power switching. The effectiveness of this jamming method against the mDT-STAP system is proved by simulations.

Author Contributions: Conceptualization, J.L. (Jiyang Li) and P.B.; methodology, J.L. (Jia Li); software, X.D.; writing—original draft preparation, J.L. (Jiyang Li); writing—review and editing, X.D. All authors have read and agreed to the published version of the manuscript.

Funding: This research was funded by Fundamentals Department of Air Force Engineering University, grant number JK2021104 and the National Natural Science Foundation of China (NSFC) (62105258).

Data Availability Statement: The authors confirm that the data and the materials supporting thefindings of this study are available within the article.

Acknowledgments: The authors would like to thank K.H Cheng, from Xi'an University of Technology.

Conflicts of Interest: The authors declare no conflict of interest.

References

1. Brenna, L.E.; Reed, I.S. Theory of adaptive radar. *IEEE Trans. Aerosp. Electron. Syst.* **1973**, *9*, 237–252. [CrossRef]
2. Melvin, W.L. A STAP overview. *IEEE Aerosp. Electron. Syst. Mag.* **2004**, *19*, 19–35. [CrossRef]
3. Klemm, R. *Principles of Space-Time Adaptive Processing*; The Institution of Electrical Engineers: London, UK, 2006.
4. Guerci, J.R. *Space-Time Adaptive Processing for Radar*, 3rd ed.; Artech House: London, UK, 2015.
5. Ward, J. Space-time adaptive processing for airborne radar. In Proceedings of the 1995 International Conference on Acoustics, Speech, and Signal Processing, Detroit, MI, USA, 9–12 May 1995.
6. Hainovich, A.M. The eignecanceler: Adaptive radar by eigenanalysis methods. *Trans. Aerosp. Electron. Syst.* **1996**, *32*, 532–542. [CrossRef]
7. Zhang, Y.; Sheng, J.S.; Liu, Y. Research into jamming to airborne radar STAP technology based on dense jamming. *Shipboard Electron. Countermeas.* **2013**, *36*, 6–8.
8. Chen, S.W.; Zhang, J.Y.; Zhou, Q.S.; Huang, Z.R. Feasibility analysis for STAP Radar scatter wave jamming. *J. Signal Process.* **2016**, *32*, 1252–1259.
9. Chen, S.W.; Zhou, Q.S.; Zhang, J.Y.; Mao, Y.X. Signal characteristic analysis of scattered wave fake clutter jamming method for STAP radar. *Acta Electron. Sin.* **2018**, *46*, 401–409.
10. Wang, K.; Zhang, J.Y.; Zhou, Q. A scattered wave jamming method against STAP base on clutter. *J. Air Force Eng. Univ.* **2021**, *22*, 62–69.
11. Wang, Y.X.; Li, X.M.; Gao, W. Dimension-reduced bi-iterative space-time adaptive processing method for airborne radar. *J. Eng.* **2019**, *2019*, 8138–8141. [CrossRef]
12. Tang, X.G.; Zhang, J.Y. Study on the principle of STAP and jamming methods for airborne phased array radar. *Electron. Des. Eng.* **2012**, *20*, 71–74+77.
13. Liu, C.S.; Zhang, Z.Y.; Tang, X.G. Modulation jamming research on airborne radar STAP technology. *Mod. Def. Technol.* **2016**, *44*, 141–147.
14. Zhao, Y.H.; Tang, J.L.; Li, J.Y.; Bi, L.H. Analysis of time-delay aliasing transmission jamming method for reduced dimension STAP airborne radar. *Syst. Eng. Electron.* **2020**, *42*, 1718–1725.
15. Chen, X.Z.; Xing, Q.J. Slow-time-frequency-modulation jamming method for STAP airborne early-warning radar. *Syst. Eng. Electron.* **2021**, *43*, 3177–3184.
16. Liu, J.C.; Wang, X.S.; Liu, Z. Preceded false target groups jamming against LFM pulse compression radar. *J. Electron. Inf. Technol.* **2008**, *30*, 1350–1353. [CrossRef]
17. Zhang, Y.R.; Li, Y.J.; Li, M.L.; Gao, M.-G.; Fu, X.-J. Suppress Jamming Technique of Multiple False Targets on Interrupted-Sampling and Non-Uniform Periodic Repeater. *Acta Electron. Sin.* **2016**, *44*, 46–53.
18. Wu, Q.; Liu, X.; Liu, J.F.; Zhao, F.; Xiao, S. A Radar Imaging Method Using Nonperiodic Interrupted Sampling Linear Frequency Modulation Signal. *IEEE Sens. J.* **2018**, *18*, 8294–8302.
19. Zhang, J.; Zhou, C. Interrupted Sampling Repeater Jamming Suppression Method based on Hybrid Modulated Radar Signal. In Proceedings of the 2019 IEEE International Conference on Signal, Information and Data Processing (ICSIDP), Chongqing, China, 11–13 December 2019; pp. 1–4.
20. Liu, Z.D.; Zhang, Q.; Li, G.M.; Li, K.M.; Wang, D. Improved Blanket Jamming Against ISAR Based on Nonperiodic Interrupted Sampling Modulation. *IEEE Sens. J.* **2021**, *21*, 430–437. [CrossRef]
21. Bao, Z.; Liao, G.S.; Wu, R.B.; Zhang, Y.H.; Wang, Y.L. 2-D Temporal-spatial adaptive clutter suppression for phased array airborne radars. *Acta Electron. Sin.* **1993**, *21*, 1–7.

22. Wang, H.; Cai, L. On adaptive spatial-temporal processing for airborne surveillance radar systems. *IEEE Trans. Aerosp. Electron. Syst.* **1994**, *30*, 660–670. [CrossRef]
23. Tong, Y.L.; Wang, T.; Wu, J.X. Improving EFA-STAP performance using persymmetric covariance matrix estimation. *IEEE Trans. Aerosp. Electron. Syst.* **2015**, *51*, 924–936. [CrossRef]